Excel@FIT 2015
http://excel.fit.vutbr.cz

AutoTaxi System Design for Aircraft

Juraj Kardoš*



Abstract
Recent studies focused on the global airline industry predict a continuous growth of passenger numbers, which will stimulate an increased demand for modern sophisticated aircraft capable of precise operations at reduced separation minima. Automation systems, such as AutoTaxi, will allow for decreased ground separation standards and a subsequent increase of throughput at airports in metropolitan areas. Such automation tools will also allow fuel savings by improving the way aircraft are operated on the ground. Except the direct operating cost, there are also associated effects, which need to be considered, namely, production of large volumes of CO2, noise pollution in the airport surroundings and an increased susceptibility to foreign object damage. This paper deals with an AutoTaxi control system for a single-aisle passenger aircraft, such as Boeing 737 series, under different operational conditions. The implemented model considers varying runway characteristics due to the atmospheric conditions and different aircraft configurations. The tire-ground interaction model has an essential impact on the ground motion model. Therefore we present detailed force and momentum equilibria analysis presented in form of equations of motion. The validation of the model was based on the turn radii comparison for multiple steering angles. Simulation results were subjected to a comparison with the analytical solution of the Ackerman drive for a tricycle vehicle and with Boeing turn radii as specified in Airplane Characteristics for Airport Planning. Obtained result suggest high-precision real-time simulation. The simulation model is assumed to be validated using actual real aircraft measured data from taxiing trials at designated international airport.

Keywords: Aircraft ground dynamics — Ground motion model — AutoTaxi

Supplementary Material: Demonstration Video — Downloadable Code

*xkardo00@stud.fit.vutbr.cz, *Faculty of Information Technology, Brno University of Technology*

1. Introduction

General Market Forecast for aircraft published periodically by Airbus states that passenger numbers will double within next 15 years, with a consequent increased demand for new airframes [1]. NASA has published a similar document in the form of the *National Plan for Aeronautics Research and Development and Related Infrastructure* [2]. Both reports high-light similar challenges and identify the automation of aircraft movements, on the ground and in the air, as a means of meeting the objectives such as the quality and affordability of aircraft, the effect on the environment, safety, security and the efficiency of the air transport system. Reduced aircraft separation due to increased demand will require a move to trajectory-based operations, novel approaches in navigation and a paradigm shift in control with new allocation of responsibilities between humans and automation.

The last thirty years have seen enormous strides made in computing capability and nowadays it is often assumed that computer size no longer determines the extent to which a model of a physical system can be constructed. Models for flight simulation, however, are subject to factors which rarely apply to other sciences which make extensive use of models. Major constraint is associated with the complex coupling between the elements which form the model - the aircraft, the aircraft's systems, the atmosphere, the airborne environment and the ground environment. It has been essential in the past to simplify these elements and to minimize the interactions between them, because of limitations imposed by computer hardware performance.

This paper provides physical model of aircraft ground motion with emphasis on tire-ground interaction model, since this interface is of essential importance in high-precision ground motion modeling. The value of the tire friction coefficient covers a wide range of potential scenarios and depends upon many factors, including: type, texture and roughness of the runway surface; type and amount of pavement contaminant, e.g. snow, ice, water; tire construction, tread design and inflation pressure; type and efficiency of an Automatic Brake System (ABS) and the aircraft ground speed. The study [3] covers wide range of friction coefficients in different operational conditions as listed above. The force and momentum equilibria analysis of an aircraft during ground motion is discussed in [4] and presents equation of motion. However, this analysis provides over-simplified model that is not suitable for realistic high-precision simulations. We extend this model by developing detailed tire-ground interaction model based on analysis in [3].

The presented model is designed for use in dynamic analysis and real-time simulation. It therefore uses mathematical expressions for on-line computation and is an alternative to earlier methods, which require the storage of large amounts of data in look-up tables containing discrete values, which are then retrieved and interpolated. In addition to real-time simulation we provide multiple options of aircraft motion visualization for better comprehension, either in form of trajectory overlay on map or as 3D rendered aircraft motion.

We also present a controller design, an essential requirement of successfully solving the automation task, which is able to steer the aircraft along a predefined path represented by series of GPX waypoints. The main function of the controller is to direct the aircraft to a dynamically changing desired heading as the individual waypoints are reached and to maintain the desired velocity with the emphasis on a well damped response.

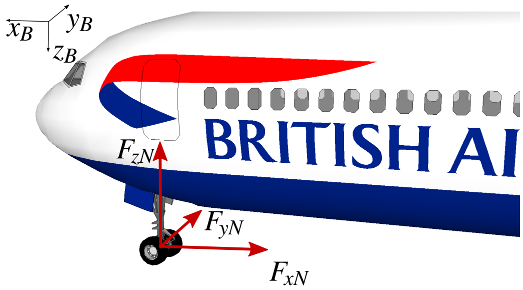

Figure 2. Forces generated at a nose tire strut.

2. Aircraft Ground Motion Model

The aircraft is modeled as single rigid body with 3 degrees of freedom (DOF). It assumes two translational DOF (motion on the plane) and rotational movement about the vertical axis. The infrastructure of the all major airports is designed so that all the runways and the taxiways are flat in order to minimize danger in ground maneuvers. This allows us to abstract the surface to a flat plane and describe movement of the aircraft over the plane as two dimensional motion.

The forces acting on aircraft are defined in Body Fixed reference frame (BFF), conventionally accepted coordinate system in avionics. Forces are illustrated in Figure 1. The equations of motion for the velocities in the body coordinate system of the aircraft are given in the form of ordinary differential equations [4]:

$$\begin{aligned} m(\dot{V}_x - V_y W_z) &= F_{xTL} + F_{xTR} - F_{xR} - F_{xL} \\ &\quad - F_{xN}\cos(\delta) - F_{yN}\sin(\delta) \\ &\quad - F_{xA} \end{aligned} \tag{1}$$

$$\begin{aligned} m(\dot{V}_y + V_x W_z) &= F_{yR} + F_{yL} \\ &\quad + F_{yN}\cos(\delta) - F_{xN}\sin(\delta) \end{aligned} \tag{2}$$

$$\begin{aligned} I_{zz}\dot{W}_z &= l_{yR}F_{xR} - l_{yL}F_{xL} \\ &\quad - l_{xR}F_{yR} - l_{xL}F_{yL} \\ &\quad + l_{xN}F_{yN}\cos(\delta) \\ &\quad - l_{xN}F_{xN}\sin(\delta) \end{aligned} \tag{3}$$

Vertical Forces Longitudinal F_{x*} and lateral F_{y*} forces (discussed bellow) are both function of vertical force F_z. The mass of the aircraft engenders gravitational force F_g acting at the center of gravity which in consequence produces the vertical forces F_{z*} acting against the gravitational force at the point of contact between the tire and the runway surface (see Figure 2).

When assuming that pitch and roll angle will remain small, since the taxiway speed of aircraft is limited, we can assume that $F_{zR} = F_{zL}$. Balancing force

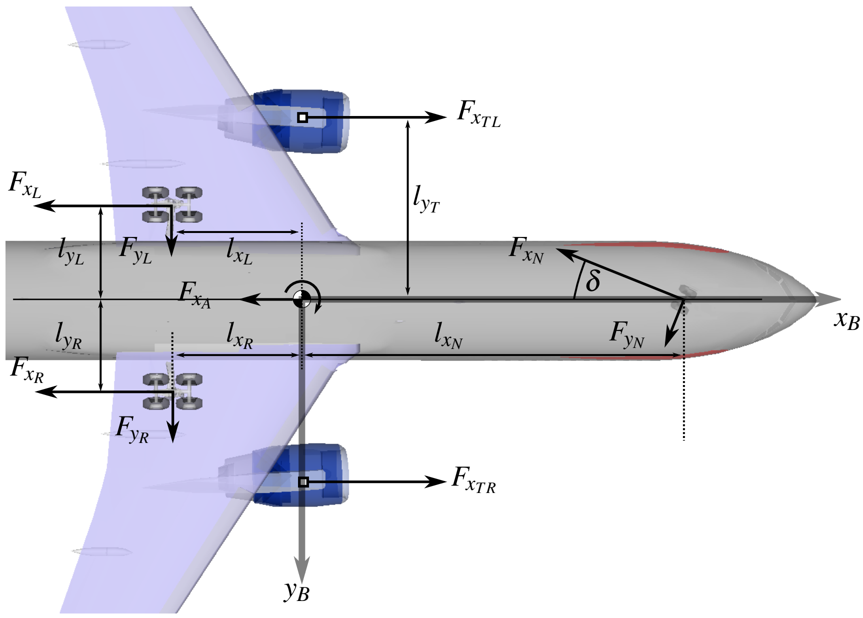

Figure 1. Schematic diagram illustrating force components acting on rigid aircraft body. Center of mass is denoted as checkerboard circle, which is reference point of BFF reference frame. Positive moment direction is shown by an arrow around C.G.

moments about axis y_B, considering the rolling friction, braking and thrust force we obtain:

$$\begin{bmatrix} 1 & 1 \\ l_{xN} - \mu_R l_{zN} & l_{xR} - (\mu_R + k_B \mu_{B_{eff}}) l_{zR} \end{bmatrix} \begin{bmatrix} F_{zN} \\ 2F_{zR} \end{bmatrix} = \begin{bmatrix} F_g \\ -l_{zT} F_{xT} \end{bmatrix} \tag{4}$$

Longitudinal Forces Longitudinal force F_x acting on wheel is composed of two components - rolling friction F_{x_R} and braking F_{x_B}.

$$F_x = F_{x_R} + k_b F_{x_b} \tag{5}$$
$$= F_z \mu_R + k_b F_z \mu_{B_{eff}} \tag{6}$$

where k_b is the proportion of brakes being used $k_b \in (0,1)$; μ_R is rolling resistance constant and $\mu_{B_{eff}}$ is a braking effectiveness coefficient.

Lateral Forces The lateral side-force F_y is created when the plane of a rolling wheel is yawed relative to the direction of motion by angle ψ_* ($*$ could be either R, L or N according to given tire of an aircraft). Two additional friction coefficients are needed to describe the lateral forces. The maximum lateral friction coefficient $\mu_{\psi_{max}}$ and the limiting lateral friction coefficient, $\mu_{\psi_{lim}}$. Coefficients differ in dependence on whether the brakes are applied. First mentioned characterizes the unbraked yawed rolling tire, the later considers the application of brakes. The model must include the effect of braking, because it can considerably reduce the maximum side-force generated by a yawed wheel. In such situations, total friction is shared between side-force generation and longitudinal deceleration. Lateral force F_y is:

$$F_y = F_z \mu_\psi \tag{7}$$

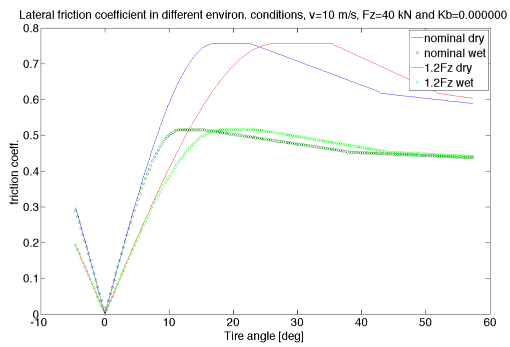

Figure 3. Lateral friction coefficient μ_ψ as a function of tire yaw angle ψ depicted in various surface conditions and different tire loads.

3. Simulation Model

Next step is transforming the mathematical model into simulation model in form of software product that is executable on appropriate computer hardware. Simulation allows us to experiment with the model and evaluate experiments that would be too expensive to perform in reality or not possible to perform at all. From the result of such simulation we can safely draw proper conclusions and have a better understanding of the system and reality. We implement our model in

Matlab and Simulink tools since such tools are considered to be industry standard because of its flexibility and capacity for quick iteration.

Our system is modeled by a system of ordinary differential equations (ODE) - equations of motion (Eq. 1, 2 and 3) based on Newtonian physics. The overwhelming majority of ODE do not have exact solution that can expressed in terms of simple functions. For this reason, we must rely on numerical methods that produce approximations to the desired solutions. In Simulink, the numerical integration is implemented by Integrator block as can be seen in Figure 4.

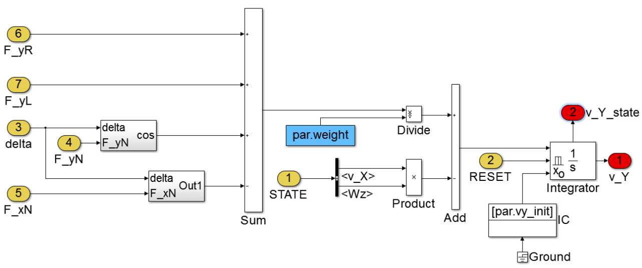

Figure 4. Simulink model of equation of motion (2).

Simulink provides rich scale of numerical methods. System programmer can select numerical solver, that computes a dynamic system's states at successive time steps over a specified time span that suits best the nature of problem in terms of desired precision, time to solution or other factors. For our purposes, we use fixed step Bogacki-Shampine solver, that computes the model's state at the next time step as an explicit function of the current value of the state and the state derivatives, using the Bogacki-Shampine Formula integration technique. Variable step solver are not efficient in our case since there is a lot of zero crossings and the variable step solvers are using too fine-grained step in order to hit the exact zero-crossing occurrence.

4. Controller Design

The design and implementation of aircraft ground motion was discussed in previous sections. We can now abstract aircraft model as dynamic system (in control theory often referred to as plant) with its inputs, outputs and create a feedback loop that will control the aircraft behavior (see Figure 5). Controller module will provide steering signals to aircraft based on some reference values that describe the desired behavior of the aircraft, namely desired velocity and target trajectory.

For heading control the objective is to steer aircraft in direction of a desired heading. The control variable is steering angle δ and the output variable is heading (yaw) Ψ. The heading error is defined as difference between desired heading and current heading of the aircraft (Figure 6):

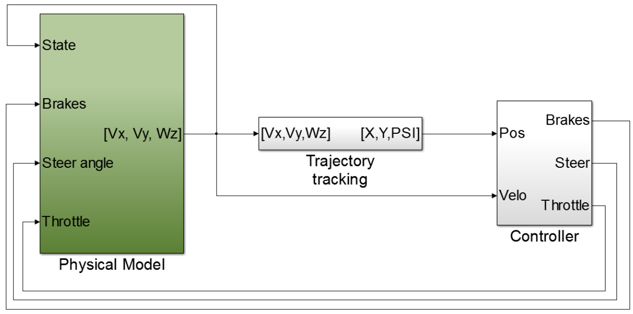

Figure 5. Simulink model of ground motion and AutoTaxi controller module.

$$\Delta_\Psi = \Psi_{des} - \Psi \tag{8}$$

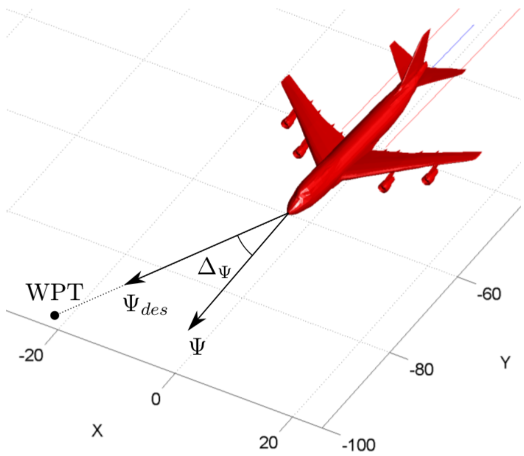

Figure 6. Desired heading Ψ_{des} to target waypoint WPT and heading error $\Delta\Psi$.

The heading controller also tries to minimize the lateral displacement. The lateral displacement of the aircraft is defined as offset e between the aircraft position P and the straight line path between two consecutive waypoints P_1 and P_2. The coordinates of the waypoints are well-known, as well as position of the aircraft. Therefore we can easily compute distances between these points forming triangle in Figure 7. From law of cosines we can compute α and consecutively lateral displacement e:

$$\alpha = \cos^{-1}\left(\frac{b^2 + c^2 - a^2}{2bc}\right) \tag{9}$$

$$e = b\sin(\alpha) \tag{10}$$

The control algorithm uses lateral displacement from the desired path to guide the vehicle back to the

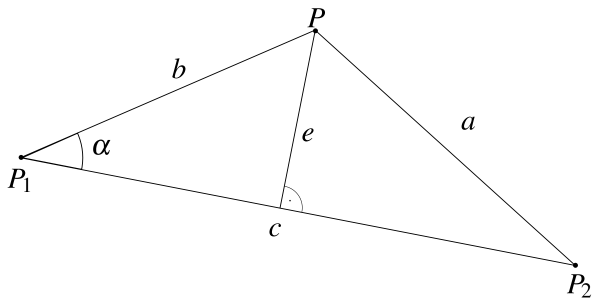

Figure 7. Geometry of lateral displacement calculations.

path, where the trajectory is assumed to be the most desirable. Aircraft is not able to develop rapid steering response in case of sharp turns so it overshoots the turn. The lateral displacement is then corrected by navigating airplane back to desired centerline trajectory.

Fusing heading and lateral displacement control is achieved by multiplying heading error $\Delta\psi$ and lateral displacement error e by respective PID gains and adding these two together to determine the steering angle of the aircraft. Because the heading error is in radians, its maximum value is π. The lateral displacement error value is in meters, and is typically much higher, thus it requires much lower gains to scale properly. The formula is expressed by equation (11) and the corresponding Simulink scheme is in Figure 8.

$$
\begin{aligned}
Steerangle = {} & \Delta\psi \cdot K_{P_H} + e \cdot K_{P_P} \\
& + \frac{d}{dt}\Delta\psi \cdot K_{D_H} + \frac{d}{dt} e \cdot K_{D_P} \\
& + \int \Delta\psi \, dt \cdot K_{I_H} + \int e \, dt \cdot K_{I_P}
\end{aligned} \tag{11}
$$

The gains are:

$$
\begin{aligned}
K_{P_H} &= 1.000 & K_{P_P} &= 0.030 \\
K_{D_H} &= 0.050 & K_{D_P} &= 0.008 \\
K_{I_H} &= 0.001 & K_{I_P} &= 0.001
\end{aligned}
$$

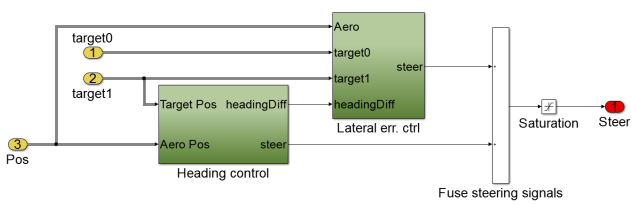

Figure 8. Simulink scheme of direction controller.

The control system must also modulate the throttle and brake to achieve a desired speed. In this case, overshoot is more important than rise time, because the vehicle cannot be permitted to overshoot a speed limit. We focus on a well damped response in case of throttle controller (Figure 9). As the controller is designed to support differential braking, allowing for sharper turns in narrow areas, the heading error was also fed to the brake controller.

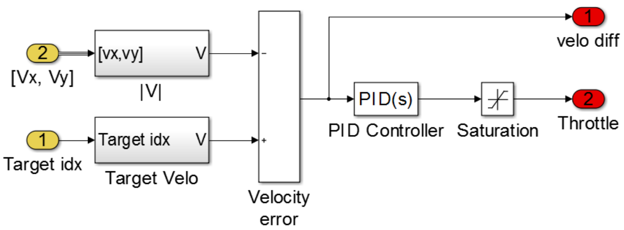

Figure 9. Simulink scheme of throttle controller responsible for velocity of the aircraft.

In our experiment, the airplane starts taxiing at stationary position and accelerates to 5 m/s. During initial taxiing phase (approximately first 150 seconds in Figure 10) airplane performs rapid turns using differential braking (trajectory can be seen in Figure 12a), therefore we observe increased error amplitude. Despite this behavior of error signal, the response of controller is rather smooth during whole taxiing trial, which is the desired behavior of velocity control.

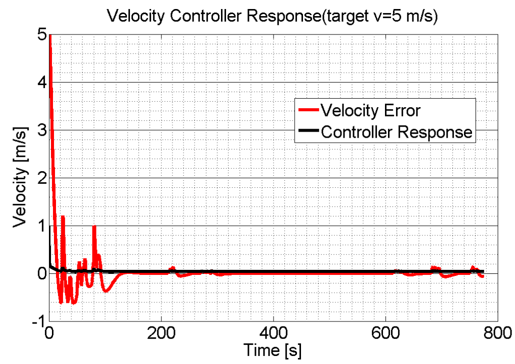

Figure 10. Controller response to velocity error signal.

5. Experiments and Model Validation

We validate our model with respect to Ackermann tricycle analytical model. Ackermann geometry avoids the need for tires to slip sideways when following the path around a curve, however, in our model modeling tire slip is of primary focus. Therefore, we cannot expect the results of our simulation to exactly match the analytical solution of Ackermann tricycle drive, but it can still provide good guidelines to simulation correctness.

Ackermann model (Figure 11) assumes that lines perpendicular to wheel axles meet at one point, denoted as ICC (instantaneous center of curvature) when vehicle is turning. As the rear wheels are fixed, this center point must be on a line extended from the

Steer angle δ [deg]	Analytical R [m]	Boeing R [m]	Simulation R [m] / Error [%]
30	28.5	28.8	30.0 / 4.00
35	24.9	25.2	25.8 / 2.33
40	22.2	22.5	22.6 / 0.79
45	20.2	20.5	20.3 / 0.99
50	18.6	18.9	18.4 / 2.66
55	17.4	17.7	16.9 / 4.55
60	16.5	16.8	16.1 / 4.54
65	15.7	16.1	15.8 / 1.77

Table 1. Comparison of turn radius R from simulation considering tire slip angle with analytical solution of Ackermann steering and Boeing specifications.

rear axle. Consequently, if the steering angle is fixed wheels are moving over circular trajectory with common center at ICC but with different radii. We evaluate turn radius for nose wheel, since it is also used in next experiment. The turn radius for nose wheel with given steer angle δ is:

$$R = \frac{l_{xR} + l_{xN}}{\sin(\delta)} \tag{12}$$

We also compare simulation results and analytical solution of nose wheel turn radii with guideline radii as specified in *Airplane Characteristics for Airport Planning* document and shown in Figure 11.

The simulation results suggest that the divergence of turn radii from analytical solution and Boeing's official document [5] is below 5% error. Our model assumes various parameters influencing the behavior of aircraft on ground. Among others, the parameters are: tire inflation pressure, runway surface contamination and tire velocity that directly influences the maximum lateral friction coefficient responsible for lateral force and thus the radius of the turn. In Table 1 we observe constant offset of turn radii of 0.3 m between analytical solution and Boeing's specification. This suggests linear model of tire skid. However, our model assumes highly non-linear model of tire lateral forces, considering the aforementioned parameters. We performed this experiment simulating dry concrete runway surface, aircraft velocity 5 m/s, tire inflated to recommended pressure 140 psi and 75% of maximum aircraft load.

These results confirm the ability of model to perform high-precision simulations. Further verification should be based on comparison with real data in order to confirm that the model is valid and corresponds to real aircraft behavior. The simulation model is assumed to be validated using actual real aircraft measured data from taxiing trials at designated international airport. However, at this stage we have no data available. Therefore we perform subsidiary experiment where we approximate taxiway guidelines on airport's runway by series of GPX waypoints. These guidelines mark the ideal trajectory for aircraft nose wheel during taxiing and as such are good reference for evaluating ability of aircraft to steer and follow predefined trajectory. The density of taxilines approximation depends on its curvature. Straight segments are approximated by two waypoints, at the beginning and at the end; turns are approximated with higher density - up to 10 meter spacial separation between consecutive marks.

Observed behavior of the aircraft during our experiment is depicted in Figure 12. The trajectory was chosen so that there are sharp turns (small radius turns), regular turns (large radius turns) and straight segments in order to evaluate simulation model in various scenarios. The airplane covered the test trajectory with maximum deviation of 2 m from predefined trajectory (Figure 12b) and deviation of 1 m/s from target velocity (Figure 12c).

The deviation from predefined trajectory (path-error) reaches its maximal value in sharp turns segment of test track. This behavior is as expected, since the turns are approximated only by straight lines represented by series of discrete points but the aircraft is moving on straight curve. As the angle between lines approximating the turn increases (which happens in small radii turns), the path-error increases as well. In turns with larger radii the path-error does not exceed deviation greater than 1 m. If we consider standard taxiway according to FAA regulation [6], the taxiway width is 22.8 m with 7.6 m wide shoulders and erosion pavement from both taxiway sides, creating a total pavement width of 53 m. The error of 2 meters from centerline is well within the safety margin. Pilots alignment with the centerline during the taxiing is also not perfect. Pilot sits in height of a couple of meters above the taxiway and his line of sight is limited to approximately 20° below horizon directly ahead. Therefore, based on this reasoning, the closest point on ground pilot can see is about 10 m ahead of him. The nose wheel is more than 2 m behind where the pilot sits. This offset between pilot's sight and actual nose wheel position makes it difficult to precisely manipulate the aircraft and some deviation from centerline is assumed.

The velocity error turns out to show greatest deviation also in sharp turns segment, reaching error amplitude of 1 m/s. Differential braking is used in sharp turns in order to increase maneuvering abilities of the aircraft. The effect of differential braking is that aircraft slows down, which is desired in sharp turns for

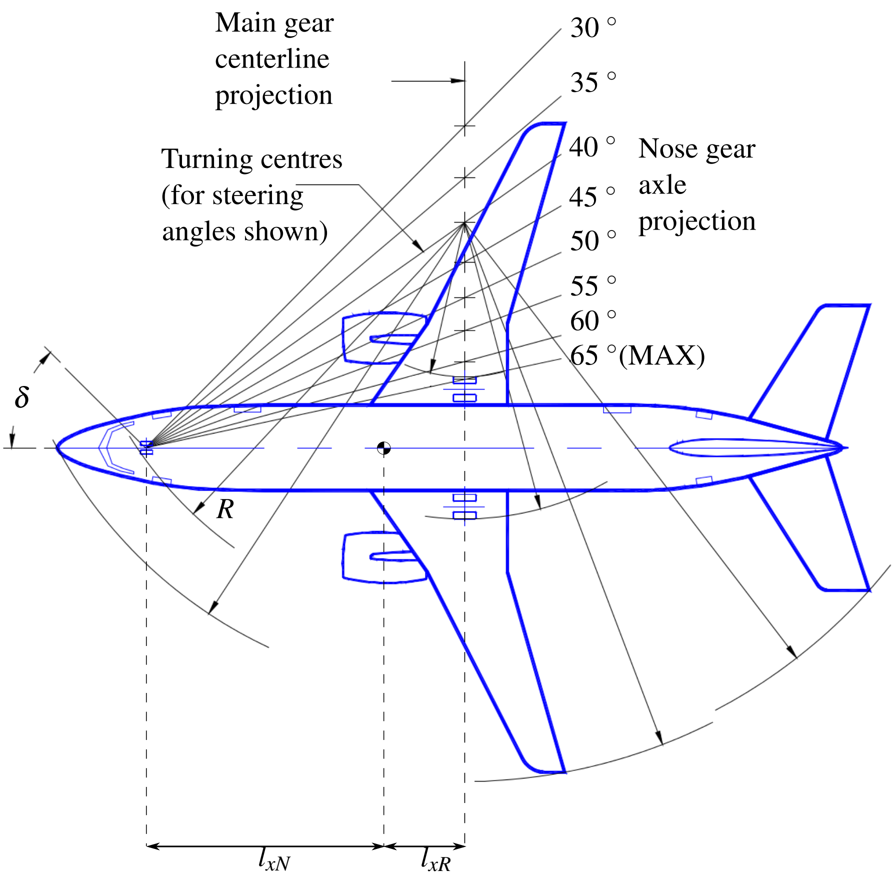

Figure 11. Ackermann tricycle steering model and turn radii for Boeing 737-400. Nose-wheel turn radius R [5].

safety reasons. In large radii turns, the error amplitude stays below 0.2 m/s.

6. Conclusions

In this paper we presented physical model of aircraft ground motion with emphasis on tire-ground interaction in different environmental and operational conditions. We also develop controller module – AutoTaxi, that is able to steer the aircraft along the predefined trajectory.

The ability of the AutoTaxi to perform realistic simulations was verified based on comparison with analytical solution of Ackermann tri-cycle model and turn radii specification by Boeing. The error is up to 4.5% in case of 60°steer angle. Evaluation of taxiway guidelines following algorithm implemented in AutoTaxi was evaluated at Ostrava-Mošnov International Airport. The simulation showed deviation from predefined trajectory below 1.4 m in standard operational conditions and 2 m in extreme rapid turn situations, which is well within safety margins.

The model is designed to be used in dynamic analysis and real-time simulation. Obtained results suggest high-precision simulation, that can be utilized for automation of ground operations at airports in metropolitan areas. Automation will lead to decreased separation minima and increased airport throughput.

Future work can be focused on developing model of selected airport and designing planning algorithm that will optimize trajectory of an aircraft from one point to another. In addition to this planning algorithm on individual aircraft level, control algorithm on global level is required, that will avoid spacial and temporal crossing of trajectories from multiple aircrafts.

References

[1] Airbus S.A.S. Global market forecast for 2014-2033, October 2014.

[2] NASA. National plan for aeronautics research and development and related infrastructure, February 2010.

[3] A.G. Barnes and T.J. Yager. Enhancement of aircraft ground handling simulation capability. 1998.

[4] J. Rankin and B. Krauskopf. Operational parameter study of aircraft dynamics on the ground. *J. Comput. Nonlinear Dynam. 5*, 2010.

[5] Boeing. 737 airplane characteristics for airport planning, September 2013.

[6] FAA. Modification of airport design standard, July 2007.

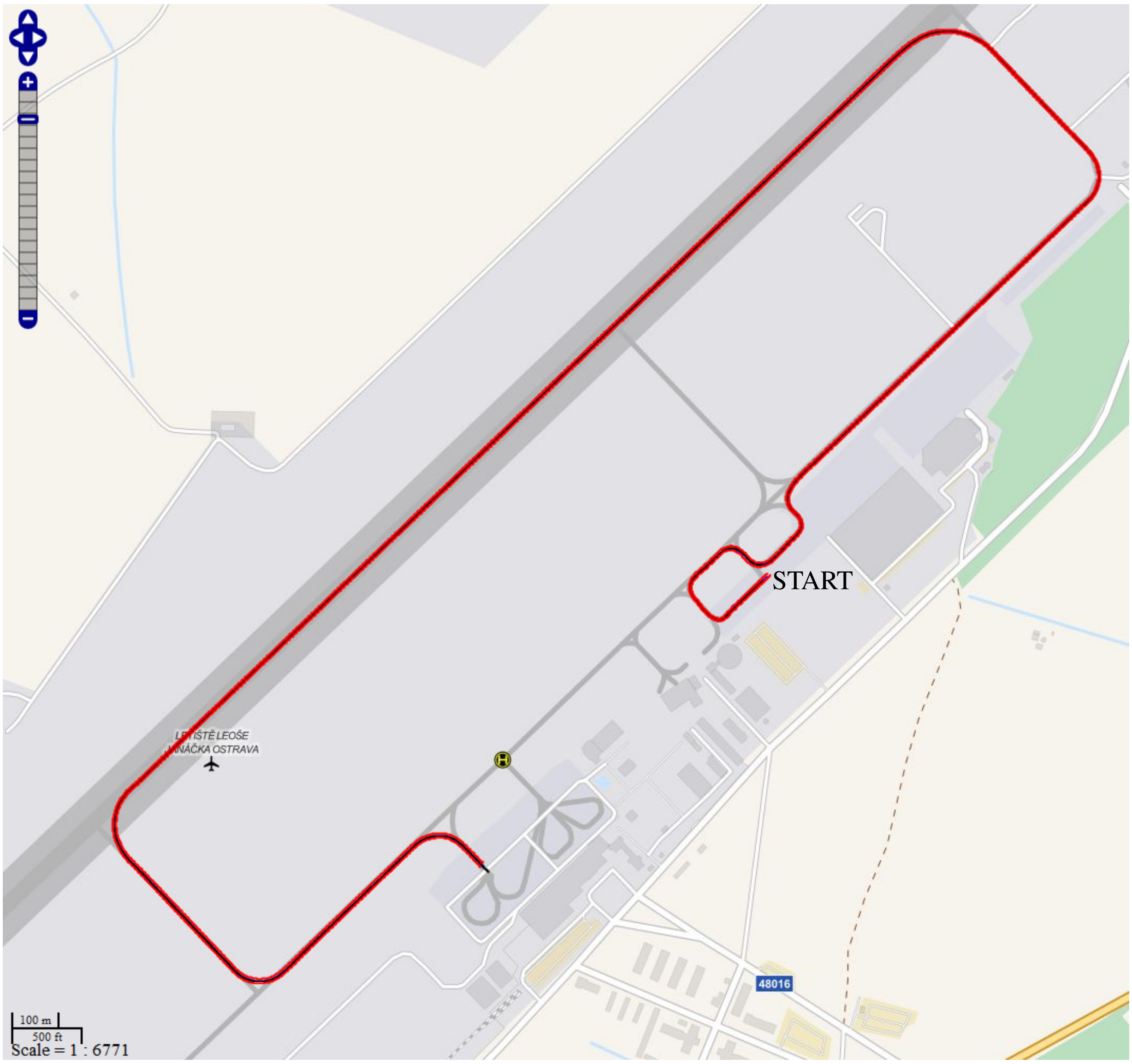

(a) Trajectory of aircraft during experiment.

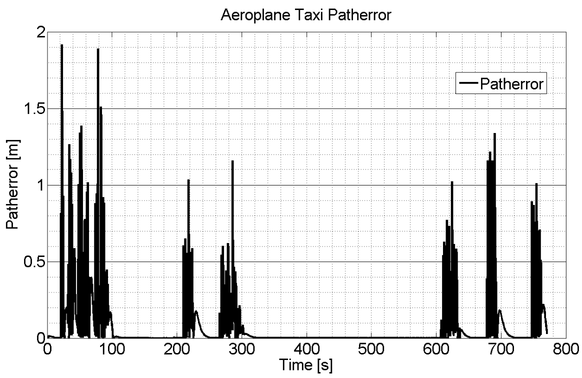

(b) Deviation from predefined trajectory.

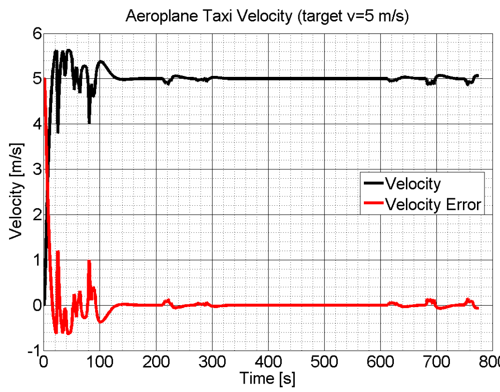

(c) Velocity behavior (target v=5m/s)

Figure 12. Evaluation of taxiway guidelines following algorithm on Ostrava-Mošnov International Airport using model of Boeing 737-400 aircraft. The aircraft follows the predefined trajectory with precision up to 1.4 m in standard operational conditions and up to 2 m in extreme, rapid turns. The velocity control is smooth, even if magnitude of velocity error increases during application of differential braking in case of sharp turns.